JOURNAL OF APPLIED ELECTROCHEMISTRY **27** (1997) 589–597

Electrochemical regeneration of Ce(IV) for oxidation of *p*-methoxytoluene

T. TZEDAKIS, A. SAVALL

Laboratoire de Génie Chimique et Électrochimie; UMR CNRS 5503, Université Paul Sabatier,
118 Route de Narbonne, 31062 Toulouse France

Received 20 December 1995; revised 20 August 1996

The development of the electrochemical oxidation of aromatic compounds on an industrial scale is hindered by the deactivation of the electrode occurring under anodic polarization. This paper presents some results on the indirect oxidation of *p*-methoxy toluene by ceric sulfate electrochemically regenerated on a platinized titanium electrode. A technique that reactivates the fouled electrode on the one hand and avoids the passivation of the electrode during electrolysis on the other hand is proposed. Methylene chloride is used to extract the organic products from the aqueous phase before electrolysis. The preparative electrolysis of anisaldehyde is performed on the laboratory scale and the results show an overall (chemical and electrochemical) yield close to 80%.

List of symbols

c	concentration (mol m^{-3} or mol dm^{-3} (M))
d_e	equivalent diameter (m)
D	diffusivity (m^2 s^{-1})
E	potential (V)
F	Faraday's constant (96 500 C mol^{-1})
I	current (A)
i	current density (A m^{-2})
$i°$	exchange current density (A m^{-2})
j	segment number
k	average mass transfer coefficient (m s^{-1})
n	electrons number
Q	charge (C)
r	recycle ratio (Φ_r/Φ)
Re	Reynolds number ($U_m d_e / \nu$)
S	electrode area (m^2)
Sc	Schmidt number (ν/D)
T	Absolute temperature (K)
U_m	average flow rate (m s^{-1})
X	conversion
α	anodic transfer coefficient
η and η_f	overall operational yield and current yield
θ	temperature (°C)
ν	kinematic viscosity (m^2 s^{-1})
ω	electrode rotation rate (rpm)
Φ	flow rate (m^3 s^{-1})
AA	*p*-methoxybenzaldehyde or *p*-anisaldehyde ($CH_3O–C_6H_4–CHO$)
AAC	*p*-methoxybenzoic acid or *p*-anisic acid ($CH_3O–C_6H_4–COOH$)
AO	*p*-methoxybenzyl alcohol or anise alcohol ($CH_3O–C_6H_4–CH_2–OH$)
DCM	methylene chloride (CH_2Cl_2)
MA	*p*-methoxytoluene or 4-methylanisol ($CH_3O–C_6H_4–CH_3$)
SCE	saturated calomel electrode

1. Introduction

Oxidation of the methyl group of toluenes leads successively to the formation of alcohol, aldehyde and acid. These products, in particular aldehydes, have many applications [1]. Oxidation can be achieved directly or indirectly. Direct anodic oxidation is performed on a platinum, gold or graphite electrode in an aqueous, organic or combined (acetonitrile, pyridine, methanol or ethanol etc.) medium [2–7]. Wendt *et al.* [6, 7] studied the direct oxidation of toluene, *p*-methoxytoluene, *p*-chlorotoluene and of 3,4,5-trimethoxytoluene on a graphite electrode in anhydrous methanol and ethanol. These authors mentioned the formation of oligomers and polymers that result in deactivation of the anodes.

The work of Abdelhedi and Bouguerra [8], who studied the effect of xylene adsorption on pretreated platinum and gold, must also be mentioned. These authors demonstrated that it was possible to decrease the adsorption rate of these compounds by adjusting the following parameters: the nature and concentration of the substrate, the nature of the electrode, its pre-treatment or its potential.

Ye and Fedkiw [9] mention the use of a Nafion® membrane, placed on a platinum electrode, which slows down its contamination by oxidation of the toluene or benzoic acid and maintains its activity for the oxidation of cations such as Fe(II) ion.

The direct anodic oxidation of benzyl alcohol, is also accompanied by polymerization reactions [2–4, 6, 7]. Brown *et al.* [2, 3] assumed that a polymer, of unknown structure, is formed from the radical cation of the alcohol before being deprotonated. This form of passivation can be avoided by adding pyridine; this base accelerates deprotonation of the cation radical

0021-891X

and directs the reaction toward formation of the aldehyde (Scheme 1).

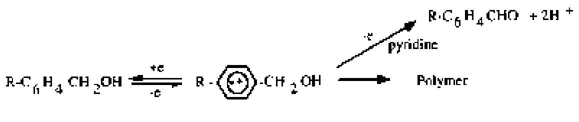

Scheme 1

The methyl group of substituted toluenes can also be oxidized selectively by using a redox couple such as Ce(III)/Ce(IV) which can be regenerated by anodic oxidation [10–12] and [13–16]. Since the solubility of the mediator in an aqueous medium is generally significantly higher than that of the organic substrate, there is a great improvement in the productivity of the electro-oxidation process.

The indirect oxidation of toluene and of *o*-chlorotoluene in solution in hexane has been performed with 0.7 M cerium perchlorate and leads to the corresponding aldehydes with yields of the order of 80% [10, 11]. In order to limit anode passivation it is necessary to reduce the concentration of the organic species to less than 150 mg dm^{-3}. However, special precautions must be taken when using perchloric acid in the presence of organic compounds due to its vigourous oxidative nature, thus prohibiting applications of the process on an industrial scale.

Ceric sulfate in a sulfuric aqueous solution was used by Kreysa and Medin [12] to oxidize *p*-methoxytoluene in dichloromethane to *p*-methoxybenzaldehyde with a yield better than 90% at a temperature of 35 °C. In the case of oxidation by manganese sulfate of several substituted toluenes, Comninellis and Plattner [17] studied the influence of the organic compound concentration on the current yield when regenerating the mediator in an aqueous solution. Salts of manganese are now being used on a pilot scale to oxidize *p*-tertiarybutyl toluene [18].

In earlier work [14–16] it was shown that the oxidation of *p*-methoxytoluene by a sulfuric aqueous solution (1 M) of ceric sulfate $Ce(SO_4)_2$ resulted in *p*-methoxybenzaldehyde selectivity of 80%. A complete kinetic study of the various consecutive stages in the oxidation of *p*-methoxytoluene was performed [15] and made it possible, by determining the various kinetic parameters, to forecast the operation of a continuously stirred liquid–liquid reactor for the oxidation of *p*-methoxytoluene into *p*-methoxybenzaldehyde [14].

The present work consists of two parts. The goal of the first part was to study the kinetics of electrochemical oxidation of *p*-methoxytoluene (or methylanisole MA) and of its oxidation products (anise alcohol AO; anisaldehyde AA and anisic acid AAC) on a rotating platinum disc electrode with a view to assessing the passivation conditions under anodic polarization. The second part looks at the indirect oxidation of MA into AA by the electrochemically regenerated Ce(IV). Schematically, the oxidation of MA by Ce(IV) can be represented by the reaction sequence shown in Scheme 2.

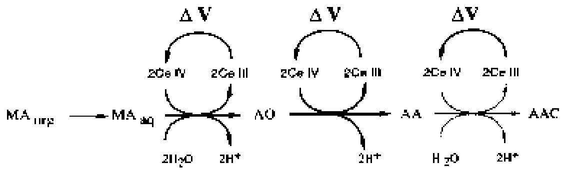

Scheme 2

The relatively high cost of cerium and the need to protect the environment make its regeneration worthwhile. Due to the passivation phenomena, a complete study of the electrochemical regeneration of Ce(IV) in the absence and then in the presence of MA or of its oxidation products was performed. Balances for preparative electrolysis of AA by indirect oxidation of MA were established and the optimization of the operation of an electrochemical reactor was also examined.

2. Experimental details

2.1 *Electrochemical kinetics*

The electrochemical kinetics of the oxidation of aromatic compounds and/or of Ce(III) in solution in 1 M sulfuric acid were studied by measuring current-potential curves on a rotating platinum disc electrode, in an isothermal reactor with a volume of 70 cm^3. The platinum electrode was carefully polished using felt and diamond paste before each recording. All the electrode potentials were measured with respect to SCE.

2.2 *Electrochemical regeneration of the mediator*

The electrochemical oxidation of the Ce(III) in an aqueous solution was studied by recording current–potential curves and by performing electrolyses in potentiostatic mode in a filter-press cell from Electro Cell AB, Sweden (Micro Flow Cell: monopolar plate and frame cell) with two compartments separated by a Nafion® 423 cationic membrane. The platinized titanium electrode had a surface area of 13 cm^2. The setup is shown in Fig. 1. The electrolytic solutions stored in the recirculating tanks (Fig. 1) were heat-regulated and recycled by pumping to the electrolytic compartments of the filter-press cell.

In the presence of organic compounds, the regeneration of Ce(IV) was performed using the same setup modified by elements 4 and 5 (Fig.1, way 1). The two-phase stirred reactor (4) was followed by a decanter (5) in which the two phases were separated. The aqueous solution of cerium in 1 M sulfuric acid and the MA phase were continuously recycled in the electrochemical and chemical reactors, respectively.

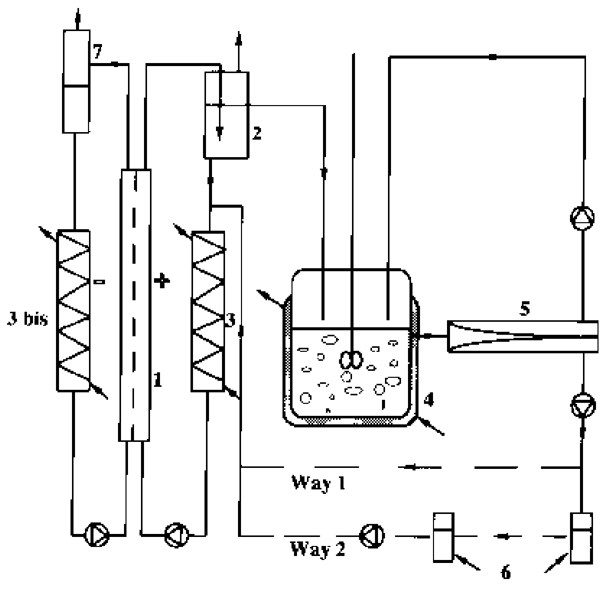

Fig. 1. Experimental setup for the electrosynthesis of anisaldehyde using Ce(III)/Ce(IV) as redox mediator. (1) Divided electrolytic cell, (2) tank of recirculating solution of cerium, (3) and (3 bis) heat exchanger, (4) continuously stirred chemical reactor, (5) horizontal decanter, (6) storage tanks and (7) catholyte recirculating tank.

2.3 *Anisaldehyde electrosynthesis*

Attempts to oxidize MA by the electrochemically regenerated Ce(IV) were made semi-continuously in the laboratory set-up which had an anisaldehyde production capacity of 150 g day^{-1} (Fig. 1). A cerium sulfate solution (0.3 M Ce(III) in 1 M H_2SO_4) free of organic substances was stored in container 6. The electrochemical reactor in which the Ce(IV) regeneration took place was fed with this solution at a flow rate Φ. The electrolyte was recycled at high speed (volumetric flow rate $\gg \Phi$) in the loop (1–2–3) which increased the mass transfer and the Ce(III) to Ce(IV) conversion rate. The solution obtained at the outlet from the electrochemical reactor, enriched with Ce(IV), was sent to the 0.7 dm^3 two-phase reactor (4) maintained at 50 °C, in which the organic phase was dispersed by vigorous stirring in the aqueous phase. Following separation in the decanter (5), the MA charged with its oxidation products (AA, AO and AAC) was directly recycled into the chemical reactor, whereas the aqueous phase obtained at the decanter outlet was purified by two extractions with dichloromethane (DCM) which was then eliminated from the aqueous phase by heating and stripping.

At the end of electrolysis, the two phases (MA and the aqueous solution) were separated and the aqueous phase was extracted with DCM. The organic phases (DCM and MA) were unified, concentrated and analysed by HPLC with anisole added as internal standard. The two products were separated on a reverse phase column (ODS C18), using an eluant made up of methanol and a solution buffered to pH 7 circulating at a rate of 1 cm^3 min^{-1}, and by creating a 30% to 100% volume methanol gradient in 6 min. The qualitative identification of the products was performed by the retention time measurement and the u.v. spectrum recording for each compound using a diode array detector. Integration of the signal for a given product, performed at the wavelength corresponding to the maximum of its molar extinction coefficient (AA and MA at 280 nm; AAC at 250 nm; AO and anisole at 270 nm) allowed its concentration to be determined following calibration.

3. Electrochemical oxidation kinetics of MA and its derivatives

3.1 *p-Methoxytoluene*

At 20 °C the oxidation of MA on a rotating platinum disc electrode (rotation rate, $\omega = 2000$ rpm) starts around 1 V and presents a plateau at 1.3 to 1.45 V. The halfwave potential is $E_{1/2} = 1.24$ V. Water oxidation starts above 1.7 V. The height of the pla teau(A) varies linearly with the concentration c of MA (mol dm^{-3}) up to a concentration of 10^{-3} mol dm^{-3} for which the maximum oxidation current density reaches 10 A m^{-2}.

$$I = 0.039\, c_{\mathrm{MA}} \tag{1}$$

For the overall reaction, the total current density, i, is given by

$$i = i^{\circ}\exp\left(\frac{\alpha nF}{RT}(E - E_{i=0})\right)$$

where i° is the exchange current density.

Logarithmic analysis of the current–potential curves gives a value for the product of the anodic transfer coefficient by the number of electrons exchanged $\alpha n = 0.34$. This value suggests a complex redox system (Scheme 3) involving the formation of the *p*-methoxybenzylic radical [13]. After the loss of a second electron the radical was transformed into a cation producing benzylic alcohol. This radical was also evidenced by electron paramagnetic resonance in the case of oxidation of the toluene and of the ethyl-2 naphthalene (Heiba *et al.* [19]).

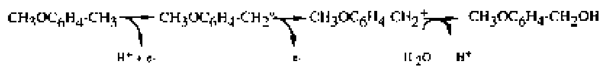

$$CH_3OC_6H_4\text{-}CH_3 \xrightarrow[H^+ + e^-]{} CH_3OC_6H_4\text{-}CH_2^{\bullet} \xrightarrow[e^-]{} CH_3OC_6H_4CH_2^{+} \xrightarrow[H_2O \quad H^+]{} CH_3OC_6H_4\text{-}CH_2OH$$

Scheme 3

When the concentration of MA in solution becomes higher than 10^{-3}M the oxidation current-potential curve shows electrode passivation. The result of this phenomenon is the partial decrease of the oxidation current above 1.3 V (Fig. 2(a), 1). Electrolysis at a potential of 1.4 V performed on a previously polished electrode shows that the current passing through the cell drops by 80% in 2 min (Fig. 2(a), 2). The current–potential curve 3, plotted after 16 min electrolysis, is similar to the solvent oxidation curve (Fig. 2(a), 4) but is slightly shifted positively.

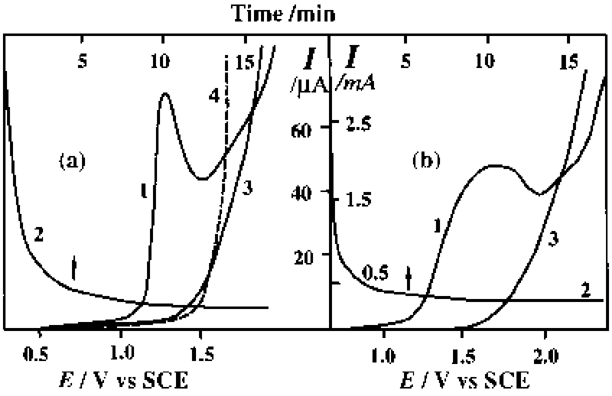

Fig. 2. Oxidation of methylanisol (a), and anise alcohol (b) on a rotating platinum disc electrode (3.14 mm^2) in 1 M H_2SO_4. Sweep potential = 5×10^{-3} V s^{-1}; rotation rate, ω = 2000 rpm; θ = 20 °C; cathode: Pt. (1) Solution saturated with MA (a) or AO (b); (2) variation of the oxidation current of organic compounds as a function of time at constant potential 1.4 V vs SCE on a polished electrode; (3) current–potential curves plotted after electrolysis; (4)(a) residual current.

3.2 *Anise alcohol*

In a sulfuric acid medium, AO can be oxidized on a platinum electrode at potentials exceeding 1.1 V and present a diffusional plateau at about 1.35 V. The halfwave potential is 1.35 V and the height of the oxidation plateau(A) is proportional to the concentration (mol dm^{-3}) of the electroactive species provided, however, that it is lower than 1 mM.

$$I = 0.0304\, c_{AO} \tag{2}$$

The comparison of the halfwave potential obtained for the oxidation of MA with that of AO shows a discrepancy of 0.11 V; consequently it is assumed that the oxidation of MA to AO takes place independently of the oxidation of AO into AA. This shows that electrolysis of the MA at an appropriately selected potential may be selectively directed to the formation of AO or AA. The AO oxidation voltammograms lead to a product anodic transfer coefficient by the number of electrons exchanged in the slow step of $\alpha n = 0.42$. For solutions containing AO at saturation concentration (13.4 g dm^{-3} at 25 °C), the current–potential curves obtained (Fig. 2(b), 1) show a maximum typical of a partial passivation by polymerization, just as for MA. Electrolysis performed at a controlled potential of 1.4 V (Fig.2(b), 2) reveals a very rapid drop in the current with time, indicative of a complete passivation of the platinum electrode after 2 min polarization. At the end of electrolysis, the current–potential curve (Fig.2(b), 3) plotted without polishing confirms electrode deactivation.

3.3 *Anisaldehyde and anisic acid*

The current–potential curves obtained on a platinum electrode for the oxidation of AA in a sulfuric acid solution (1 M) at various concentrations show that the latter is practically inactive electrochemically. However, its presence in solution tends to increase the potential of oxygen evolution ($\Delta E = 50$ mV for 0.6 mM of AA solution) which suggests passivation of the electrode due to an adsorption and/or a slight oxidation of the AA on the electrode.

The results obtained with a sulfuric solution (1 M) saturated with anisic acid show a complete absence of electrochemical activity of AAC on a platinum electrode.

4. Electrochemical regeneration of the mediator

The purpose of this study was to define the experimental conditions for regenerating the mediator Ce(IV) at maximum rate in the absence or in the presence of organic compounds.

4.1 *In the absence of organic compounds*

The current–potential curves for the oxidation of the cerium ion in an aqueous solution without any organic compounds plotted on a platinized titanium electrode in the filter press cell are given in Fig. 3. Curve 2 shows that the oxidation of the Ce(III) takes place at potentials higher than 1.1 V and a diffusion pseudo-plateau is observed around 1.65 V. The potential of oxygen evolution on Ti–Pt is lower than in the case of platinum (~1.8 V). The oxidation current density of Ce(III) at 20 °C is of the order of 700 A m^{-2} for a $Ce_2(SO_4)_3$ concentration of 0.15 M (concentration close to saturation: 0.18 M at 20 °C in 1 M H_2SO_4) and an anolyte and catholyte circulation rate of 30 dm^{3}h^{-1} (0.15 m s^{-1}). The electrochemical reaction speed is therefore limited by the mass transport process due to the low solubility of cerium sulfate $Ce_2(SO_4)_3$.

To increase the Ce(III) oxidation current density, electrolyses were performed on a platinized titanium electrode at a controlled potential (1.65 V) at tem-

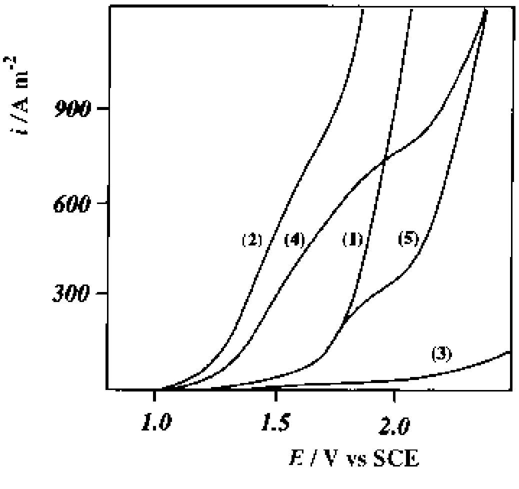

Fig. 3. Current–potential curves on a platinized titanium anode in the filter-press cell for Ce(III) oxidation in 1 M H_2SO_4; cathode: Pb; sweep potential = 4.2×10^{-3} V s^{-1}; θ = 22 °C; $\Phi_{Anolyte} = \Phi_{Catholyte}$ = 30 dm^3 h^{-1}; $S_{Anode} = S_{Cathode}$ = 13 cm^2. (1) residual current; (2) $Ce_2(SO_4)_3$: 0.15 M; (3) $Ce_2(SO_4)_3$: 0.15 M saturated with MA or AA; (4) $Ce_2(SO_4)_3$: 0.15 M after two extractions of MA and AA with CH_2Cl_2; (5) H_2SO_4:1 M saturated with CH_2Cl_2 (~0.15 M).

peratures between 25 and 53 °C with the experimental setup described in Section 2.2 (Fig. 1). The anolyte ($100\,cm^3$) was a sulfuric acid solution of Ce(III) sulfate whereas the catholyte only contained sulfuric acid. The current was recorded and at the end of electrolysis (20 min) the potentiometric titration of Ce(IV) by Mohr's salt can be used to determine the current efficiency (η_f) value defined by Relation 3:

$$\eta_f = \frac{(\text{number of moles of Ce(IV)})F}{Q} \qquad (3)$$

where Q is the charge (C) and F is Faraday's constant ($96500\,C\,mol^{-1}$).

It was assumed that the total cerium concentration in the anolyte had not decreased significantly, due to the high value of the protons/cerium concentration ratio and to the high mobility of the proton. The results given in Fig. 4 show an increase of the Ce(III) oxidation current of approximately 100% if the temperature is raised from 25 to 53 °C. The corresponding variation of the mass transfer coefficient with the temperature is shown in the insert. The current yield of the Ce(III) oxidation fell from 98% to 87% when the temperature was increased from 25 to 53 °C. The balance is anodic oxygen evolution.

To summarize, the electrochemical regeneration of Ce(IV) from Ce(III) at a concentration of 0.3 M can be achieved at 50 °C and a current density greater than $1500\,A\,m^{-2}$ with current yields of about 90%.

4.2 *In the presence of organic compounds*

If the electrolyte is charged with MA or its oxidation products, the electrochemical regeneration of Ce(IV) on a Ti–Pt anode is practically impossible. The current–potential curve obtained on Ti–Pt with a solution of $Ce_2(SO_4)_3$ at 0.15 M in 1 M sulfuric acid saturated with MA or AA is given in Fig. 3 (curve 3). Comparison with curve 2 in the same figure shows that the electrode is completely inhibited, and only the oxidation of the solvent takes place at potentials higher than 2.5 V. Deactivation of the electrode during its anodic polarization results from the formation of polymers with low conductivity.

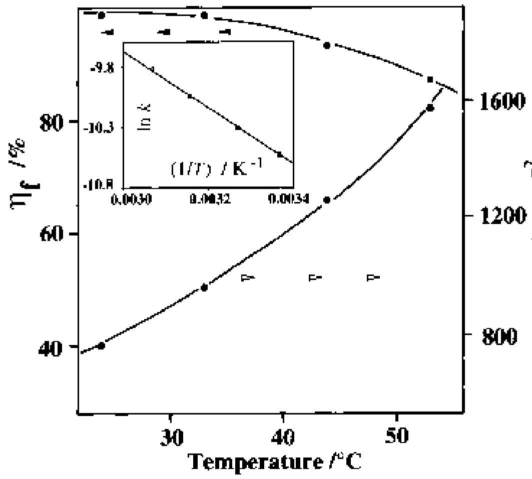

Fig. 4. Electrochemical regeneration of Ce(IV) on a platinized titanium anode in a filter-press cell (Electrocell AB microflow). Current density and current efficiency as functions of temperature. $100\,cm^3$ of 1 M H_2SO_4 with $Ce_2(SO_4)_3$: 0.15 M; Anodic potential = 1.65 V vs SCE; electrolysis duration = 1200 s; $\Phi_{Anolyte} = \Phi_{Catholyte} = 30\,dm^3\,h^{-1}$; $S_{Anode} = S_{Cathode} = 13\,cm^2$; cathode: Pb. Inset: mass transfer coefficient in $m\,s^{-1}$ of Ce(III) as a function of temperature.

Attempts to electrosynthesize anisaldehyde by indirect oxidation of MA were made using the setup shown in Fig. 1 with elements: 1, 2, 3, 3bis, 4, 5 (way 1) and 7. The sulfuric aqueous solution obtained at the decanter outlet was saturated with MA. During potentiostatic mode electrolysis ($E = 1.8$ V) of this solution, the Ce(III) (0.3 M) oxidation current decreased to zero after a few minutes. In contrast, for galvanostatic electrolyses (I = 1A), only the water was oxidized at the anode; the electrolytic solution remained colourless and the cerium regeneration faradaic yield was practically null.

It should be noted that vitreous carbon or solid platinum electrodes behaved in the same way as the platinized titanium electrode. Furthermore, if the polarity between the electrodes was reversed for a few seconds, no long-lasting depassivation occurred.

4.3 *Depassivation study*

In order to prevent contamination of the electrode, the liquid–liquid extraction technique was used to purify the aqueous solution charged with organic compounds. The solvent chosen for extraction was dichloromethane (DCM) because it is miscible with MA and AA and does not exhibit miscibility gaps with these two substrates. Furthermore, it is only slightly soluble in the sulfuric aqueous solution (0.15 M at 20 °C) containing the cerium and chemically it is relatively inert with respect to the mediator. However, the current-potential curve for the oxidation of a sulfuric acid solution saturated with DCM (Fig. 3, curve 5) shows that DCM can be oxidized on a Ti–Pt electrode; the diffusion type current is not negligible with respect to the limit current obtained under the same experimental conditions (curve 2) with a 0.3 M solution of Ce(III). It is therefore vital to eliminate the DCM from the aqueous phase before recycling aqueous solution in the electrochemical reactor.

4.3.1 Study on rotating platinum disc. The oxidation current of Ce(III) in the aqueous phase was monitored on a rotating platinum disc in potentiostatic mode before and after the addition of MA or its oxidation products (Fig. 5 inset). The electrode was brought to a potential of 1.9 V, which corresponds to the diffusion plateau of Ce(III) on Pt, in the absence of organic compounds. When the current had stabilized, a volume of $2\,cm^3$ MA (or AA) was added to the solution (100 ml). The Ce(III) oxidation current decreased, and then vanished completely when the stirring rate was increased.

A current–potential curve plotted for these conditions is identical to curves 3(a) or (b) in Fig. 2. After decantation, the aqueous phase underwent a series of extractions, each time with 5 cm^3 DCM (E1 to E5, Fig. 5 inset). Each extraction was followed by decantation and then elimination of the DCM by heating to 50 °C. At the fifth operation, the Ce(III) oxidation current was once again identical to that obtained before the addition of the organic compound. The current–potential curve plotted after these operations suggests oxidation of the Ce(III) on Pt (Fig. 2 of [14]).

To summarize, electrolysis of an aqueous solution saturated with MA or AA leads to complete blocking of the electrode; however, this problem can be eliminated by extracting the organic substrates. The shapes of the current-potential or current-time curves return to what they were before passivation. Extraction with DCM completely extracts the MA and AA and completely reactivates the surface of the electrode.

4.3.2 Study on the platinized titanium electrode. The previous study was repeated on a platinized titanium electrode to determine the number of steps of aqueous phase liquid–liquid extraction by DCM required to prevent passivation of this electrode type and perform Ce(III) oxidation in optimum conditions. Curve 1 in Fig. 5 shows the change in current as a function of time for the oxidation of a 1 M sulfuric aqueous solution of Ce(III) at a concentration of 0.3 M, saturated with MA or AA (10 cm^3 of organic compound for 100 cm^3 aqueous phase). The current passing when electrolysis was performed at a controlled potential of 1.65 V was practically nil. The aqueous phase, saturated with MA or AA, was then submitted to the first extraction in a decanting flask with an equivalent volume of DCM. The stirred reactor and the filter press cell were thoroughly cleaned, then assembled again, and the aqueous phase was recycled in the reactor. The current–potential curve obtained with this solution, similar to curve 4 in Fig. 3, shows Ce(III) oxidation coupled with DCM oxidation; the potential of oxygen evolution was shifted to anodic values of 0.5 V with respect to a solution containing only Ce(III) (curve 2, Fig. 3). The dissolved DCM was eliminated by heating and the aqueous solution was electrolysed again at 1.65 V. Curve 2 in Fig. 5 shows that the current stabilized at 150 $A\,m^{-2}$ and then tended to increase slightly over time. After 30 min electrolysis, the potentiometric titration of the Ce(IV) gave a calculated faradaic yield η_f of 55%. The cerium solution still contained enough MA or AA whose oxidation poisoned the electrode and led to a very average current yield.

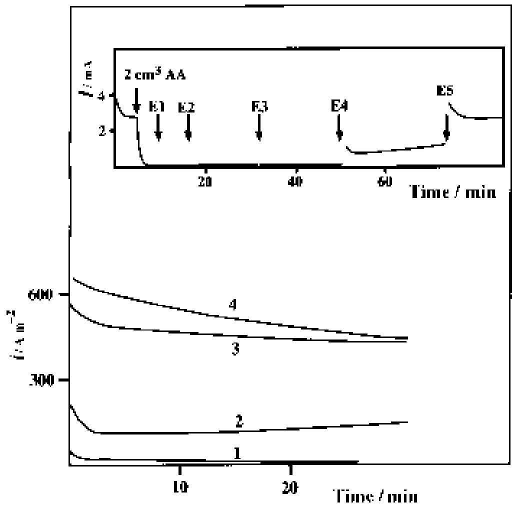

Fig. 5. Electrolysis current at controlled potential for Ce(III) oxidation as a function of time and extraction stage by DCM. 100 cm^3 of $Ce_2(SO_4)_3$ 0.15 M in 1 M H_2SO_4; $\theta = 25\,°C$; filter-press cell (Electrocell AB microflow); anode: Ti–Pt; cathode: Pb; $E = 1.65$ V vs SCE; $\Phi_{Anolyte} = \Phi_{Catholyte} = 30\,dm^3\,h^{-1}$; $S_{Anode} = S_{Cathode} = 13\,cm^2$. (1) MA or AA at saturation; (2) after 1st extraction (100 cm^3 of DCM); (3) after two extractions (100 cm^3 of DCM); (4) without organic products in solution. Inset: Anode: Pt rotating disc electrode; $S = 3.14\,mm^2$; 20 cm^3 of 0.15 M $Ce_2(SO_4)_3$ solution in 1 M H_2SO_4 saturated by anisaldehyde; $E = 1.9$ V vs SCE; rotation rate $\omega = 2000$ rpm; cathode: Pt. (E1–E5) Number of extraction stages of the aqueous phase with 5 cm^3 of DCM. Current recorded after total elimination of DCM.

A second operation (extraction–stripping–electrolysis) was performed under the same conditions as above. The current time dependence (curve 3) was practically the same as that obtained in the case of a cerrous sulfate solution (Fig. 5, curve 4) without any organic compounds. The observed difference (6%) corresponds to the decrease in the Ce(III) concentration obtained during the first electrolysis. Moreover, HPLC analysis of the aqueous solution that had undergone the two extractions with DCM did not detect the presence of MA ($c_{MA} < 5 \times 10^{-5}$ M); the concentration of AA present was 1.7×10^{-5} M. These values are compatible with those given by Kramer *et al.* [11] in the case of oxidation of toluenes by cerium perchlorate; however, they are lower than those observed by Comninellis and Plattner during the oxidation of substituted toluenes by manganese sulfate [17]. Furthermore, for the electrolyses performed in 3 and 4 (Fig. 5), titration of the Ce(IV) formed led to current efficiencies equal to 98 and 99%, respectively.

To summarize, it can be considered that a 0.3 M sulfuric aqueous solution in Ce(III) that has been saturated with *p*-methoxytoluene or with anisaldehyde in the chemical reactor is capable of undergoing electrochemical regeneration, without any decrease in the anode activity after two extractions with DCM and distillation of this solvent.

5. Electrosynthesis of anisaldehyde

The attempts to oxidize MA by the electrochemically regenerated Ce(IV) were made on the set-up described in Fig. 1 (way 2). The electrochemical regeneration of the Ce(IV) was completely separated from the *p*-methoxytoluene chemical oxidation reaction. Furthermore, in order to avoid any contact between the anode and the organic compounds dissolved in the aqueous solution, the latter was purified by two discontinuous extractions with DCM. This solvent saturated the aqueous phase and was then eliminated by distillation. In galvanostatic mode the anode potential, monitored during electrolyses for a total of 24 h, did not increase significantly ($\Delta E < 0.01$ V).

The overall yield is defined by Equation 4 and the results of the runs are given in Table 1:

$$\eta = \frac{\left(\begin{array}{c}\text{number of moles}\\ \text{of organic compound formed}\end{array}\right) F\, n}{Q} \qquad (4)$$

where the electrons number n is 2 for AO, 4 for AA and 6 for AAC.

Analysis performed showed that the anisic acid was formed with a yield not greater than 4%. The anise alcohol is an intermediate obtained under the conditions described in Table 1 with a yield of between 7 and 17%. This yield did not vary significantly as a function of the current density (attempts 3, 4, 5, 6 and 7, Table 1) nor as a function of the temperature (attempts 1, 2 and 4, Table 1).

Increase in temperature from 36 °C to 50 °C enhanced the formation of anisaldehyde, since its yield increased from 50 to 68% (attempts 1, 2 and 4). These results are in line with those obtained during the chemical reaction selectivity study [15] between Ce(IV) and MA performed discontinuously at laboratory scale. The increased solubility of the MA with temperature rise was responsible for this change.

The anisaldehyde yield increased slightly from 67 to 76% when the current density increased from 500 to 1538 A m^{-2} (attempts 3 to 6, Table 1). This change can be explained by the increase in the concentration of Ce(IV) contained in the solution introduced into the chemical reactor. Assuming that in the continuously stirred liquid-liquid reactor the MA transfer flow to the aqueous phase was the same for these attempts, it can be accepted that an increase in the concentration of Ce(IV) in the introduced aqueous solution enhances the formation of AA. For the highest current density (attempts 7) a significant drop in the aldehyde yield was observed due to the competition with the oxygen released on the anode. Attempt 8, performed with a Ce(III) flow rate of half that of attempt 4, confirmed these results (86% AA yield).

The result for the regenerated Ce(IV) systematically indicated a loss of between 5 and 15%, attributed on the one hand to the formation of unidentified secondary products [15] and, on the other hand, to the fall in the electrochemical regeneration yield of Ce(IV) during electrolyses at high temperature (Fig. 4).

6. Optimizing the electrochemical regeneration of Ce(IV)

Since it was necessary to purify the electrolytic solution before regenerating the Ce(IV), only the virtually complete conversion of Ce(III) into Ce(IV) in the electrochemical reactor could make the process viable; the electrochemical regeneration conditions must therefore be defined.

6.1 *Assessment of the mass transfer coefficient*

Generally the conversion rate obtained with a single pass through a continuously supplied electrochemical cell is low: for example, in the case of an ElectrocellAB microflow cell operating at limiting current, the conversion rate X reached in one pass does not exceed 2%. The decrease in the electrolyte flow rate results in an increase in the conversion rate, but leads to a fall in the anodic limiting current due to the decrease of the mass transfer coefficient. Conversion can be improved by recycling the solution in the electrochemical reactor (loop 1, 2, 3, Fig. 1). The mass transfer coefficient k and the overall conversion rate then increase appreciably [20, 21].

For galvanostatic electrolyses and in a continuously-fed reactor with recycling, it is necessary to determine the current value to be imposed to obtain the required conversion rate with a yield close to 100%. The calculations below were developed for the case of an ElectrocellAB filter press electrochemical reactor with an effective surface area of 100 cm^2 (MP cell) and for which it was assumed that the mass transfer correlation established for the Electro Syn

Table 1. Results of preparative electrolyses of anisaldehyde

Attempts	i /A m^{-2}	$X_{\mathrm{Ce(III)}}$ (*a*) / %	$\theta_{\text{liq–liq}}$ *reactor* / °C	Q / C	η / % *AA*	*AO*	*AAC*
1(c)	769	–	36	7620	50	16.0	–
2(c)	769	–	45	7620	65	12.6	–
3	500	3.5	50	4680	67	16.5	1.7
4(c)	769	–	50	7620	68	17.2	–
5(c)	1153	8.3	50	11250	71	7.0	–
6	1538	11.1	50	14400	76	15.4	1.3
7	1923	13.2	50	18000	65	16.1	4.2
8(b)	769	11.8	50	7200	86	8.2	0.9

Anode : Ti–Pt; aqueous phase: 0.7 dm^3 of 1 M H_2SO_4 with 0.15 M $Ce_2(SO_4)_3$; 0.4 dm^3 in stirred liquid–liquid reactor; V_{MA}:0.1 dm^3; impeller rate: 400 rpm; $\theta_{\mathrm{Anolyte}} = \theta_{\mathrm{Catholyte}} = 55 \pm 2$ °C; flow rate Φ of Ce(III) = 2 dm^3 h^{-1}; recycling condition : ($\Phi+\Phi_r$): 30 dm^3 h^{-1}; cathode: Pb; catholyte: 1 M of H_2SO_4; $S_{\mathrm{Anode}} = S_{\mathrm{Cathode}}$ = 13cm^2; electrolyses duration: 120–130 min. (a) Electrochemical conversion measured by potentiometric titration of Ce(IV); (b) flow rate Φ of Ce(III) 1 dm^3 h^{-1}; (c) AAC not assayed.

cell is valid [20 and 22]. The maximum permissible flow rate for each of this reactor's compartments is 600 $dm^3 h^{-1}$ and the correlation giving the mass transfer coefficient k as a function of the Reynolds (Re) and Schmidt (Sc) numbers has the form:

$$k = 5.57 \frac{D}{d_e} Re^{0.4}\, Sc^{0.33} \qquad (5)$$

where d_e is the equivalent diameter and D the diffusion coefficient.

Using the diffusion coefficient $D_{Ce(III)} = 5 \times 10^{-10}$ $m^2 s^{-1}$ [23, 24], and the following experimental relationship giving the kinematic viscosity of the sulfuric aqueous solution (1 M),

$$\nu = 1.1 \times 10^{-5} \theta^{-0.55} \qquad (6)$$

for Ce(III) at 0.3 M as a function of the temperature θ [16], it is possible to determine k at 25 °C from Relation 5.

The variation of the mass transfer coefficient with the absolute temperature T is then determined from

$$k = 6.72 \times 10^{-2} \exp - (19200/RT) \qquad (7)$$

Relationship 7 is established experimentally [16] in the case of the microflow cell (Fig. 4, inset) and is assumed to be valid in the case of the MP filter-press cell from the same manufacturer.

6.2 *Regeneration current*

Assuming that the MP reactor is continuously supplied at a flow rate Φ with a sulfuric solution (1 M) of Ce(III) at a concentration $c°$ (Fig. 6). For the calculation, the surface area S of the anode was divided into N segments of unit surface area S_j. In each segment j the concentration c was considered to be approximately constant. A fraction of the solution obtained at the reactor output was recycled and the total flow rate of the solution in the reactor was $\Phi_r + \Phi$. The molar flux balance (at point M; inset 2, Fig. 6) is written:

$$c° + rc = (1 + r)c_1 \qquad (8)$$

where r is the recycle ratio $= \Phi_r / \Phi$.

In the case of limiting current (concentration at the electrode = 0), the output concentration c of the Ce(III) is related to the concentration c_1 at the input to the first segment by

$$c = c_1 \exp\,[- k\, S/\Phi(1 + r)] \qquad (9)$$

The concentration c_1 is then given by

$$C_1 = \frac{c°}{1 + r - r \exp\,[- k\, S/\Phi(1 + r)]} \qquad (10)$$

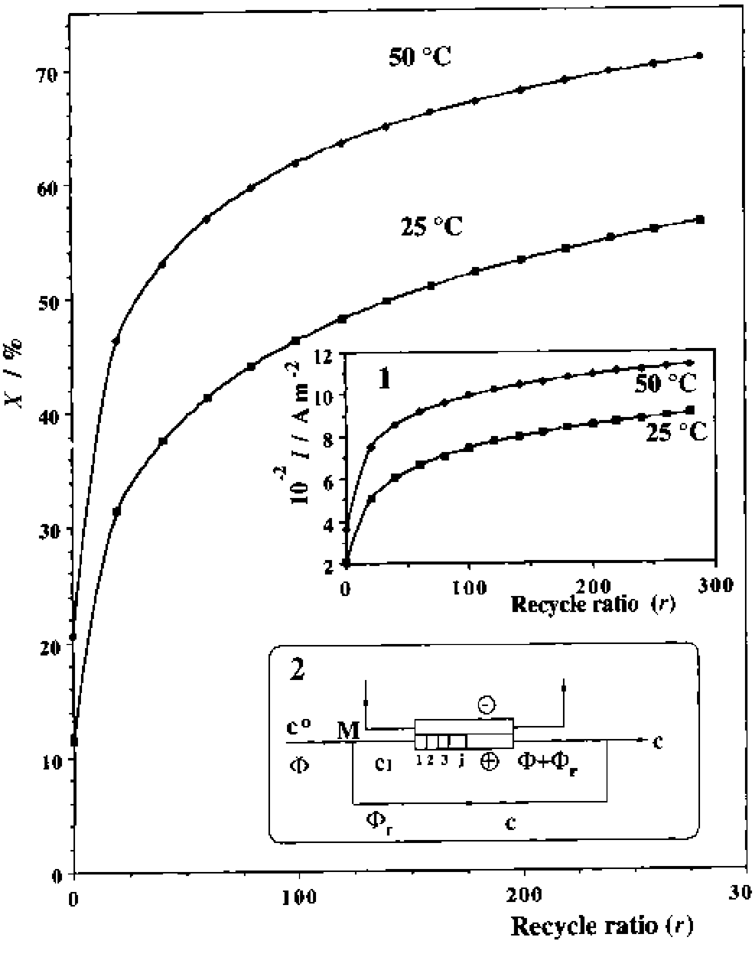

Fig. 6. Variation of the calculated conversion of the Ce(III) as a function of the recycling ratio at 25 and 50 °C in the case of the ElectrocellAB MP cell. $S_{Anode} = S_{Cathode} = 0.01$ m^2; anode: Ti–Pt; $Ce_2(SO_4)_3$: 0.15 M; H_2SO_4:1 M; $\Phi = 2$ $dm^3 h^{-1}$. Inset 1: variation of the calculated current as a function of recycling ratio at 25 and 50 °C. Inset 2: Schematic representation of the anodic compartment of the MP type filter press reactor divided into segments.

The variation of the Ce(III) concentration in this segment can be obtained, using Faraday's law, by calculating the current ($I_{\lim\ 1} = F\ c_1\ k\ S_1$). For a segment *j*, the output concentration c_j is expressed by

$$c_j = c_{j-1} - \frac{I_{\lim\ j}}{F\Phi(1+r)} \tag{11}$$

The total current to be imposed is then calculated from

$$I = \sum_{j=1}^{j=N} I_{\lim,j} \tag{12}$$

Figure 6 gives the theoretical Ce(III) conversion *X* obtained in the continuously fed MP filter press reactor with a solution of Ce(III) at 0.3 M in sulfuric acid at 1 M at a rate of 2 $\mathrm{dm^3\,h^{-1}}$, as a function of recycle ratio *r* for two temperatures. For each recycle ratio, the optimum current density is estimated (inset 1, Fig. 6).

It should be noted that the theoretical current densities obtained for the MP reactor are compatible with the experimental current densities obtained in the case of the microflow cell. After correction of the geometric area ratio between the two reactors the agreement is satisfactory ($\Delta i < 5\%$).

The curves show that the Ce(III) conversion *X* at the MP reactor output increases with *r* and that the increase in the conversion is slowed down for a recycle rate higher than 100. At 25 °C, 56% of the Ce(III) is converted to Ce(IV) for $r = 280$ (maximum permissible flow for MP reactor). Increasing the temperature to 50 °C gives a conversion rate of 71%, due to the increase in the mass transfer coefficient. The improvement made by raising the temperature is still not sufficient to reach complete conversion of Ce(III), hence the need to reduce the flow rate or increase the number of reactors. Calculations have been made according to the same principle with two electrochemical reactors of the same type placed in series with recycle [16]. The results show that a solution initially containing Ce(III) at 0.3 M continuously supplying two reactors in which a recycle rate of 300 was applied, undergoes a conversion of more than 90% at a temperature of 50 °C.

7. Conclusion

An anodically polarized Ti–Pt electrode loses its activity on contact with an aqueous solution saturated with MA. This is a result of adsorption and polymerization reactions of the aromatic substrate and its derivatives. However, a previously contaminated electrode regains its activity if the organic products are extracted below a threshold of 5×10^{-5} M. Moreover, it is possible to avoid anode deactivation provided that two extractions are performed on the aqueous phase with DCM and then this solvent is eliminated by flash distillation before recycling the mediator in the electrolysis cell. Under these conditions Ce(IV) can be regenerated with a faradaic yield as high as 90% by electrolysis at 50 °C of a sulfuric aqueous solution at a current density of 1600 $\mathrm{A\,m^{-2}}$. During electrolysis of this type the anode potential does not change significantly.

The results of preparative electrolysis show anisaldehyde can be synthesized with an overall yield, including the faradaic and chemical yields, of the order of 80%. The previously demonstrated need [16] to operate at high temperatures to facilitate the dissolution of the MA is confirmed by the preparative electrolyses. Indeed the AA yield increased by 20% when the temperature was increased from 35 to 50 °C. By operating with a volume excess of MA with respect to the aqueous phase, it is possible to protect the AA formed against oxidation. The amount of anisic acid formed is always lower than 4% AAC.

Acknowledgement

We would like to thank Isochem Co. (Gennevilliers, France) and Electricité de France for their financial support during this work.

References

[1] H. G. Franck and J. W. Stadelhofer 'Industrial Aromatic Chemistry', Springer-Verlag, Berlin (1988).

[2] O. R. Brown, S. Chaudra and J. A. Harrison, *J. Electroanal. Chem.*, **34** (1972) 505.

[3] *Idem, ibid.* **38** (1972) 185.

[4] L. Coche and J. C. Moutet, *Electrochim. Acta* **30** (1985) 1063.

[5] E. A. Mayeda, L. L. Miller and J. F. Wolf, *J. Am. Chem. Soc.* **94** (1972) 6812.

[6] H. Wendt and S. Bitterlich, *Electrochim. Acta* **37** (1992) 1951.

[7] H. Wendt, S. Bitterlich, E. Lodowicks and Z. Liu, *ibid.* **37** (1992) 1959.

[8] R. Abdelhedi and M. L. Bouguerra, *ibid.* **35** (1990) 273.

[9] J. -H. Ye and P. S. Fedkiw, *J. Electrochem. Soc.* **141** (1994) 1483.

[10] N. Ibl, K. Kramer, L. Ponto and P. Robertson, *A.I.Ch.E. Symp. Series* **75** (1979) 45.

[11] K. Kramer, P. M. Robertson and N. Ibl, *J. Appl. Electrochem.* **10** (1980) 29.

[12] G. Kreysa and H. Medin, *ibid.* **16** (1986) 757.

[13] S. Torii, 'Electrooxidation of Alkylbenzene. Side-Chains In Electro-organic Syntheses, Part I', Kodansha and VCH, Tokyo, Weinheim (1985); pp. 75–95.

[14] T. Tzedakis, and A. Savall, *Chem. Engng. Sci.* **46** (1991) 2269.

[15] *Idem, Ind. Eng. Chem. Res.* **31** (1992) 2475.

[16] T. Tzedakis, Etude de procédés d'électro-oxidation indirecte de composés aromatiques par l'emploi d'ions métalliques. Doctorat de l'Université Paul Sabatier, Toulouse (1989).

[17] Ch. Comninellis and E. Plattner, *J. Appl. Electrochem.* **17** (1987) 1315.

[18] P. Vaudano, *Chimia* **46** (1992) 103.

[19] E. I. Heiba, R. M. Dessau and W. J. Koehl, *J. Am. Chem. Soc.* **191** (1969) 6830.

[20] F. Cœuret and A. Storck, Eléments de Génie Electrochimique, Lavoisier, Paris 1984.

[21] D. J. Pickett 'Electrochemical reactor design', Elsevier, Amsterdam (1979).

[22] L. Carlsson, B. Sandegren and D. Simonsson, *J. Electrochem. Soc.* **130** (1983) 342.

[23] A. T. Kuhn and T. H. Randle, *J. Chem. Soc. Faraday Trans.* **1** (1983) 1741.

[24] T. H. Randle and A. T. Kuhn, *Electrochim. Acta* **31** (1985) 739.